Nihashi T, Yatsuya H, Hayasaka K, Kato R, Kawatsu S, Arahata Y, Iwai K, Takeda A, Washimi Y, Yoshimura K, Mizuno K, Kato T, Naganawa S, Ito K:	Direct comparison study between FDG-PET and IMP-SPECT for diagnosing Alzheimer's disease using 3D-SSP analysis in the same patients. Radiat Med 25: 255-262, 2007	Radiat Med	25	255-262	2007
伊藤健吾	J-ADNIの先行研究としてのJ-COSMIC, SEAD-Japan	Cognition and Dementia	6	281-286	2007
加藤隆司，伊藤健吾，新畑　豊	「脳神経，核医学」　特集　高齢者における画像診断　～高齢者にみられる画像変化を中心に～	日獨医報	52	460-469	2007
岡村信行、谷内一彦、工藤幸司	アミロイドイメージングの進歩	Dementia Japan	20	216-225	2007
古川勝敏、温　世栄、岡村信行、工藤幸司、荒井啓行	アルツハイマー病におけるシナプス障害	Dementia Japan	20	253-261	2007
荒井啓行、工藤幸司	病理像を画像化する分子神経イメージング法によるAlzheimer病の早期診断　－日本でのBF-227の開発と臨床応用	医学のあゆみ	220	404-408	2007
Kudo Y, Okamura N, Furumoto S, Tashiro M, Furukawa K, Maruyama M, Itoh M, Iwata R, Yanai K, Arai H	2-(2-[2-Dimethylamino- thiazol -5-yl] ethenyl) -6-(2-[fluoro]ethoxy) benzoxazole: A novel PET agent for in vivo detection of dense amyloid plaques in Alzheimer's disease patients.	J Nucl Med	48	553-561	2007
Okamura N, Furumoto S, Funaki Y, Suemoto T, Kato M, Ishikawa Y, Ito S, Akatsu H, Yamamoto T, Sawada S, Arai H, Kudo Y, Yanai K	Binding and safety profile of novel benzoxazole derivative for in vivo imaging of amyloid deposits in Alzheimer's disease.	Geriatr Gerotol Int	7	393-400	2007
Furumoto S, Okamura N, Iwata R, Yanai K, Arai H, Kudo Y	Recent advances in the development of amyloid imaging agents	Curr Top Med Chem	7	1773-1789	2007
Okamura N, Furumoto S, Arai H, Iwata R, Yanai K, Kudo Y	Imaging amyloid pathology in the living brain.	Curr Med Imaging Rev	4	56-62	2008
Okamura N, Funaki Y, Tashiro M, Kato M, Ishikawa Y, Maruyama M, Ishikawa H, Meguro K, Iwata R, Yanai K.	In vivo visualization of donepezil binding in the brain of patients with Alzheimer's disease.	Br J Clin Pharmacol.	65(4)	472-479	2008
Suzuki M, Okamura N, Kawachi Y, Tashiro M, Arao H, Hoshishiba T, Gyoba J, Yanai K.	Discrete cortical regions associated with the musical beauty of major and minor chords.	Cogn Affect Behav Neurosci.	8	126-131	2008
Jia F, Mobarakeh JI, Dai H, Kato M, Xu A, Okuda T, Sakurai E, Okamura N, Takahashi K, Yanai K.	Blocking histamine H(1) improves learning and mnemonic dysfunction in mice with social isolation plus repeated methamphetamine injection.	J Pharmacol Sci.	107	167-174	2008

Tashiro M, Sakurada Y, Mochizuki H, Horikawa E, Maruyama M, Okamura N, Watanuki S, Arai H, Itoh M, Yanai K.	Effects of a sedative antihistamine, D-chlorpheniramine, on regional cerebral perfusion and performance during simulated car driving.	Hum Psychopharmacol.	23	139-150	2008
岡村信行，谷内一彦，古本祥三，工藤幸司，古川勝敏，荒井啓行.	[11C]BF-227を用いた脳アミロイド斑の画像化.	臨床放射線	53(7)	876-884	2008
谷内一彦，岡村信行，田代学	レビュー：ポジトロン医学と創薬.	PET Journal	1	21-23	2008
谷内一彦、須原哲也	序にかえて「脳の核医学分子イメージング」	臨床放射線	53(7)	845-848	2008
谷内一彦、岡村信行	分子イメージング研究におけるPETの現状と今後の展望：アルツハイマー病を中心に	Medical Now	65	p8-12	2009
古本祥三、工藤幸司	アミロイド斑の可視化によるアルツハイマー病の早期診断	Isotope News	655	2-6	2008
荒井啓行、工藤幸司	アルツハイマー病治療の現状と近未来像	細胞	40	17-20	2008
荒井啓行、古川勝敏、工藤幸司	アルツハイマー病バイオマーカー開発の現状	Alzheimer's Disease Neuroimaging Initiative. Human	19	12-17	2008
工藤幸司、古本祥三、岡村信行	アミロイド画像化用プローブ	日本臨床	66	300-306	2008
岡村信行、谷内一彦、古川勝敏、荒井啓行 工藤幸司	アミロイドイメージング　PET	日本臨床	66	288-292	2008
岡村信行、古本祥三、工藤幸司	アミロイドイメージング	分子精神薬理	2	188-190	2008
石井賢二	ポジトロン断層法（PET）の現状と展望	Medical Technology	37	241-247	2009
石井賢二	MCIの画像診断を考える−PIB−PETによる画像診断の将来−	老年精神医学雑誌	20	55-60	2009
石井賢二	アミロイドイメージング	Clinical Neuroscience	27	108-109	2009
石井賢二	前頭側頭型認知症の機能画像診断	Geriatric Medicine	46	1096-1103	2009
石井賢二	アミロイドイメージングのインパクトと今後の展望	映像情報Medical	40	730-732	2008
加藤隆司，旗野健太郎，伊藤健吾	認知症診療における核医学のシンポと課題　−アミロイドイメージング−特集　核医学の最前線.	映像情報Medical	40	976-979	2008

伊藤健吾	PET/SPCETによるアルツハイマー病の診断を目的とした臨床試験	臨床放射線	53	885-892	2008
伊藤健吾,加藤隆司,新畑豊,鷲見幸彦	アルツハイマー病の早期画像診断	BIOClinica2008	23(8)	714-720	2008
伊藤健吾	アルツハイマー病と脳核医学—最近	東北脳循環カンファレンス	14	5-9	2008

研究成果の刊行物・別刷

Geriatr Gerontol Int 2007; 7: 393–400

ORIGINAL ARTICLE: BIOLOGY

Binding and safety profile of novel benzoxazole derivative for *in vivo* imaging of amyloid deposits in Alzheimer's disease

Nobuyuki Okamura,[1] Shozo Furumoto,[2] Yoshihito Funaki,[3] Takahiro Suemoto,[4] Motohisa Kato,[1] Yoichi Ishikawa,[3] Satoshi Ito,[1] Hiroyasu Akatsu,[5] Takayuki Yamamoto,[5] Tohru Sawada,[4] Hiroyuki Arai,[6] Yukitsuka Kudo[2] and Kazuhiko Yanai[1]

[1]Department of Pharmacology, Tohoku University Graduate School of Medicine, [2]Tohoku University Biomedical Engineering Research Organization (TUBERO), [3]Division of Radiopharmaceutical Chemistry, Cyclotron and Radioisotope Center, Tohoku University, [6]Center for Asian Traditional Medicine, Department of Geriatrics and Gerontology, Tohoku University School of Medicine, Sendai, [4]BF Research Institute, Osaka, and [5]Fukushimura Hospital, Toyohashi, Japan

Background: *In vivo* detection of amyloid deposits in the brain is potentially useful for early diagnosis of Alzheimer's disease (AD) and tracking the efficacy of anti-amyloid therapy.

Methods: To develop an amyloid-binding agent for positron emission tomography, we screened over 2600 compounds.

Results: We found benzoxazole derivatives as candidate compounds for *in vivo* amyloid imaging probes. One of these agents, 2-(2-[2-dimethylaminothiazol-5-yl]ethenyl)-6-(2-[fluoro]ethoxy)benzoxazole (BF-227), displays high binding affinity to Aβ fibrils. BF-227 binding increased linearly with increasing Aβ fibril formation. In temporal and hippocampal AD brain sections, BF-227 selectively bound to amyloid plaques. In contrast, no staining was evident in the cerebellum. Compared with the previously reported compound BF-168, ^{18}F-labeled BF-227 displayed selective *in vivo* labeling of amyloid fibrils and rapid washout from white matter areas in an Aβ-injected rat model. An acute and subacute toxicity study of BF-227 indicated sufficient safety for clinical use as a positron emission tomography probe.

Conclusions: These findings suggest that BF-227 is feasible as an *in vivo* imaging probe of amyloid deposits in AD patients.

Keywords: Alzheimer's disease, amyloid, positron emission tomography, senile plaques.

Introduction

Progressive deposition of senile plaques (SP) and neurofibrillary tangles (NFT) is a critical event in the pathogenesis of Alzheimer's disease (AD). These lesions precede the presentation of clinical symptoms of dementia.[1] For early or presymptomatic diagnosis of AD, non-invasive detection of these lesions using positron emission tomography (PET) is a potentially

Accepted for publication 22 August 2007.

Correspondence: Dr Nobuyuki Okamura MD PhD, Department of Pharmacology, Tohoku University Graduate School of Medicine, 2-1 Seiryo-machi, Aoba-ku, Sendai 980-8575, Japan. Email: oka@mail.tains.tohoku.ac.jp

doi: 10.1111/j.1447-0594.2007.00430.x

useful technique.[2] To achieve successful *in vivo* imaging using PET, sensitive and selective contrast agents to these lesions are needed. Congo red and thioflavin T have represented attractive lead compounds as developing amyloid-imaging agents, because these compounds selectively bind to β-pleated sheet structures and are commonly used for histochemical staining of SP. However, the permeability of these compounds through the blood–brain barrier (BBB) is extremely limited.[3] The chemical structure must thus be optimized to provide appropriate lipophilicity without changing the binding properties to amyloid. Thioflavin T derivatives without any positive charge show high permeability of the BBB. One of these compounds, 6OH-BTA-1 (PIB), has been applied in a human PET study and enabled successful detection of early AD patients.[4] Another compound, 2-(1-[6-[<2-fluoroethyl><methyl>amino]-2-naphthyl]ethylidene) malononitrile (FDDNP), is extremely lipophilic and can easily penetrate the BBB, and specifically binds to both SP and NFT in AD brain sections.[5] After i.v. injection of FDDNP, greater accumulation was observed in SP- and NFT-rich areas of the human brain.[6] Although validation is still required as to whether retention of these agents in the neocortex truly reflects levels of amyloid deposition, such findings suggest the potential usefulness of this technique for early diagnosis of AD.

We have previously demonstrated a novel series of compounds including 6-(2-fluoroethoxy)-2-(2-[4-methylaminophenyl]ethenyl)benzoxazole (BF-168) and (2-[4-methylaminophenyl]ethenyl)-5-fluorobenzoxazole (BF-145) as promising candidates for *in vivo* imaging probes of SP.[7–9] These benzoxazole derivatives demonstrate high binding affinity for Aβ aggregates and high BBB permeability, suggesting potential utility as *in vivo* amyloid-binding agents. However, for the application of these compounds to clinical PET studies, the pharmacokinetic properties and pharmacological safety of these molecules requires improvement. This study describes the characterization of an optimized benzoxazole derivative, 2-(2-[2-dimethylaminothiazol-5-yl]ethenyl)-6-(2-[fluoro]ethoxy) benzoxazole (BF-227), as a candidate *in vivo* amyloid-imaging agent in humans.

Methods

Preparation of the compounds

BF-168, BF-227 (Fig. 1) and the precursor compounds for ^{18}F-labeled agents were custom-synthesized by Tanabe R & D Service (Osaka, Japan). Synthesis of (^{18}F)BF-168 was performed by reacting 2-(4-methylaminophenyl)-6-(2-tosyloxyethoxy) benzoxazole (Tanabe R & D Service) with (^{18}F)KF and Kryptofix 222 (Merck, Darmstadt, Germany) in acetonitrile at 80°C for 20 min, as described previously.[8] Radiosynthesis of (^{18}F)BF-227 was performed using the same method. After subsequent high-performance liquid chromatography (HPLC) purification, ^{18}F-labeled compounds were obtained (Fig. 1). Details of the radiosynthetic methods will be described elsewhere.

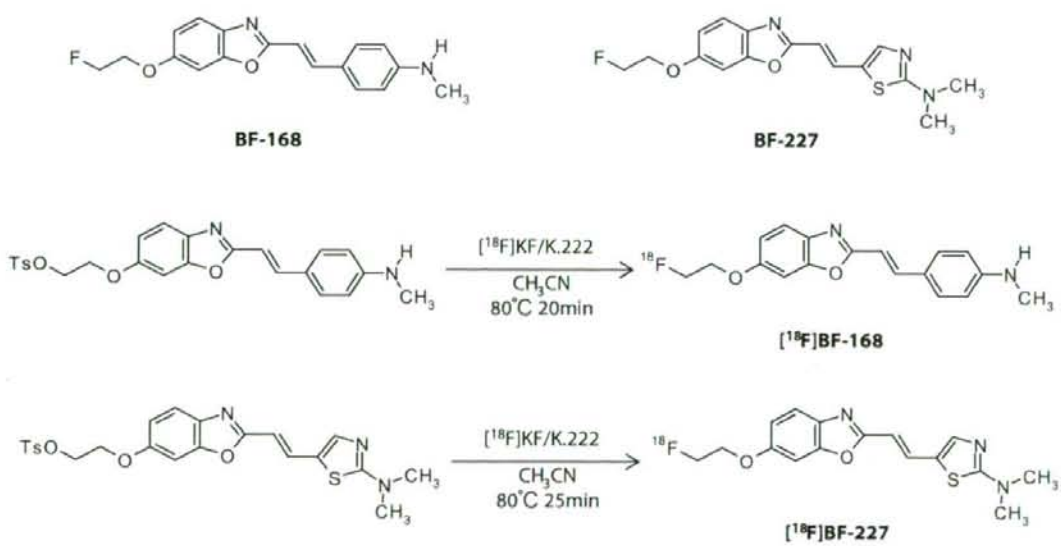

Figure 1 Chemical structures and radiosynthesis of BF-168 and BF-227.

In vitro *binding assays*

Binding affinities of the compounds for synthetic Aβ aggregates were examined as described previously.[7] Briefly, solid-form Aβ1–40 (Peptide Institute, Osaka, Japan) was dissolved in 10 mmol/L potassium phosphate buffer (pH 7.4) and incubated at 37°C for 72 h. The binding assay was performed by mixing aggregated Aβ1–40 with the appropriate concentration of ^{18}F-labeled BF-227, unlabeled BF-227 and dimethyl sulfoxide. After incubation for 10 min at room temperature, the binding mixture was filtered using a cell harvester (Model M-24; Brandel, Gaithersburg, MD, USA) and filters containing bound ^{18}F ligand were counted using a γ-counter. The dissociation constant (K_d) of BF-227 was determined by Scatchard analysis.

Fluorometric analysis of BF-227 binding with Aβ fibrils was performed using the following method. A total of 20 μmol/L of Aβ1–40 or Aβ1–42 (Peptide Institute) in 50 mmol/L of potassium phosphate buffer (pH 7.4) was incubated at 37°C on a Vibrax VXR shaker (IKA, Cincinnati, OH, USA) at 0.56 *g*. Before fluorometric analysis, Aβ solutions were sonicated for 3 min at 45 kHz using a VS-100III ultrasonic cleaner (Iuchi, Osaka, Japan). In fluorometry, Aβ1–40 and Aβ1–42 solutions at 0, 4, 8 and 24 h after the start of incubation were mixed with the same volume of BF-227 solution (5 μmol/L final concentration). After determination of the optimal excitation wavelength for the mixture of BF-227 and Aβ, fluorescence spectra were measured using a Gemini XS microplate spectrofluorometer (Molecular Devices, Sunnyvale, CA, USA). In addition, fluorescence spectra for the mixture of 5 μM BF-227 and different concentrations of Aβ1–40 or Aβ1–42 (0.15, 0.5 1.5, 2.5, 5 and 10 μmol/L final concentrations) at 96 h after incubation (fibrillar Aβ) were measured using the microplate spectrofluorometer. The same measurements were also performed using Aβ1–40 and Aβ1–42 with no incubation (non-fibrillar Aβ). All measurements were performed in triplicate.

Neuropathological staining

Postmortem brain tissues from an autopsy-confirmed AD case (69-year-old man) were obtained from Fukushimura Hospital (Toyohashi, Japan). Experiments were performed under the regulations of the Ethics Committee of BF Research Institute. Serial sections (6-μm thick) from paraffin-embedded blocks of temporal cortex and cerebellum were prepared in xylene and ethanol. Before staining, quenching of autofluorescence was performed as described previously. Quenched tissue sections were immersed in 100 μmol/L of BF-227 solution for 10 min or 0.01% 1-bromo-2,5-bis(3-carboxy-4-hydroxystyryl)benzene (BSB) solution containing 50% ethanol for 30 min. Sections stained with BF-227 were then dipped briefly into water and rinsed in phosphate-buffered saline (PBS) for 60 min before coverslipping with Fluor Save Reagent (Calbiochem, La Jolla, CA, USA), and examined using an Eclipse E800 microscope (Nikon, Tokyo, Japan) equipped with a V-2A filter set (excitation 380–420 nm, dichroic mirror 430 nm, longpass filter 450 nm). Sections stained with BSB were dipped briefly in tap water and then in 50% ethanol, then washed in PBS for 60 min before coverslipping, followed by fluorescent microscopy using a BV-2A filter set (excitation 400–440 nm, dichroic mirror 455 nm, longpass filter 470 nm). In addition, adjacent sections were immunostained using monoclonal antibody (mAb) against Aβ (6F/3D; Dako A/S, Glostrup, Denmark). After pretreatment with 90% formic acid for 5 min, sections were immersed in blocking solution for 30 min and then incubated for 60 min at 37°C with 6F/3D at a dilution of 1:50. Following incubation, sections were processed by the avidin–biotin method using a Pathostain ABC-POD(M) Kit (Wako, Osaka, Japan) and diaminobenzidine tetrahydrochloride. Fluorescence intensity of three different brain slices stained with BF-227 was analyzed by defining regions of interest (ROI) and measuring the intensity of fluorescence within gray and white matter using Lumina Vision software (Mitani, Fukui, Japan). Ratios of gray matter ROI to white matter ROI were calculated as an indicator of stainability and statistical comparisons were performed using ANOVA and Scheffe post-hoc tests.

Labeling of amyloid deposits in Aβ-injected rat model

Aβ1–40 (Peptide Institute) was dissolved at 500 μmol/L in 50 mmol/L potassium phosphate buffer and incubated at 37°C for 4 days. An Aβ-injected rat model was created as described previously.[10] Briefly, Wistar rats (male, 200–250 g, SLC, Shizuoka, Japan) were injected with Aβ peptides unilaterally and potassium phosphate buffer contralaterally into each amygdala using a stereotaxic instrument (Model 5000, David Kopf, Tujunga, CA, USA). Injection coordinates measured from the bregma and skull surface (anteroposterior, −3.0 mm; mediolateral, ±5.0 mm; dorsoventral, −8.8 mm) were determined based on a stereotaxic atlas.[11] A volume of 1.0 μL was administered over 2 min using a microsyringe and glass cannula (tip diameter, 170–250 μm). At 3 days after injection of Aβ and vehicle, (^{18}F)BF-168 (72.8 MBq) or (^{18}F)BF-227 (58.9 MBq) were administered into the femoral vein of anesthetized rats. Rats were killed by decapitation at 180 min postinjection and the brains were removed and frozen. An OTF cryostat (Bright Instruments, Huntingdon, UK) was used to cut 30-μm thick frozen sections, which were then dried and exposed to a BAS-III imaging plate for 18 h. Autoradiographic images were obtained using a BAS2000 scanner system

(Fuji Film, Tokyo, Japan). After autoradiographic examination, the same sections were stained with thioflavin-S to confirm the presence of amyloid plaques.

Toxicity study in mice

A non-GLP (good laboratory practice) toxicity study was performed using female and male ICR mice (weight, 22–32 g). The Ethics Committee of BF Research Institute approved the protocol for these experiments. Animals were kept in a temperature-controlled environment (21.2–23.5°C) with a 12-h light–dark cycle and ad libitum access to food and water. In the acute toxicity study, animals were divided into one control group and three treated groups, with 10 animals (five males, five females) in each group. The control group received injection of vehicle alone, while each treated group received i.v. injection of BF-227 solution in doses of 0.1, 1 or 10 mg/kg. Animals were observed for 8 days after administration to identify any changes in general behavior or bodyweight. In the subacute toxicity study, animals were divided into one control group and two treated groups (2.5 and 25 μg/kg), with 10 animals (five females, five males) in each group. The control group received injection of vehicle alone and each treated group received i.v. injection of BF-227 solution for 14 days (once daily). Animals were weighed at 3, 7, 9 and 14 days after administration. At the end of the experiment, animals were sacrificed and examined at autopsy. Selected organs (brain, heart, liver, lung and kidney) were removed, weighed and examined microscopically by a pathologist.

Results

Binding characteristics of BF-227 for Aβ fibrils

In vitro binding assay indicated that BF-227 shows high binding affinity for Aβ fibrils. K_d for Aβ1–40 fibrils was 1.0 ± 1.4 nmol/L, comparable to previously reported levels for amyloid imaging agents[12] (Fig. 2). Binding ability of BF-227 to Aβ was also examined by fluorometric analysis, as BF-227 is highly fluorescent. In the mixture of BF-227 and Aβ peptides, fluorescence intensity of BF-227 increased as Aβ1–40 (Fig. 3a) and Aβ1–42 (data not shown) incubation time advanced. BF-227 fluorescence also increased in a linear manner with increasing concentrations of fibrillar Aβ1–42 (Fig. 3b) or Aβ1–40 (data not shown), but did not increase in mixture with non-fibrillar Aβ. These results suggest that degree of BF-227 binding reflects the amount of Aβ fibril formation.

Neuropathological staining in AD brain sections

Neuropathological examination using BF-227 indicated that amyloid plaques were clearly stained with BF-227 in AD brain sections (Fig. 4a). In particular, cored plaques stained brightly with this compound. This staining pattern correlated well with Aβ immunostaining in adjacent sections (Fig. 4b). BF-227 staining was further compared to staining using BSB, a Congo red derivative. In contrast to clear staining of SP and NFT with BSB (Fig. 4c), BF-227 primarily stained SP, with faint staining of NFT. Preferential binding of BF-227 to SP rather than NFT represents a similar characteristic to the previously reported compound BF-145. BF-227 staining was subsequently performed in three different regions (temporal lobe, hippocampus and cerebellum) of an AD brain. In temporal (Fig. 5a) and hippocampal (Fig. 5b) sections, cored plaques stained brightly with BF-227. In contrast, no staining was evident in the cerebellum (Fig. 5c). Fluorometric measurement of these brain sections indicated that overall level of stainability in the cerebellum differed significantly from that in the temporal cortex and hippocampus (Fig. 5d), suggesting the binding specificity of this compound to AD pathology.

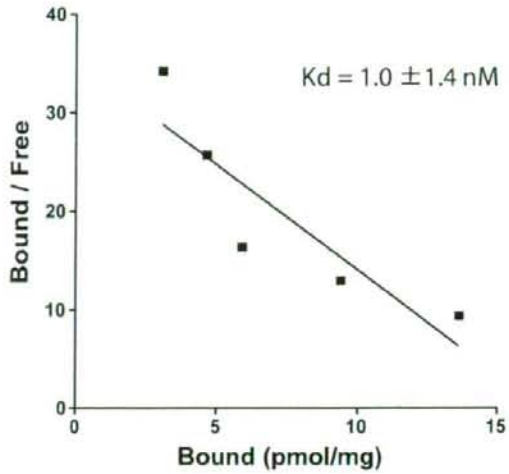

Figure 2 Scatchard plots of (^{18}F)BF-227 binding to synthetic Aβ fibrils.

Intravenous administration of ^{18}F-labeled agents in Aβ-injected rat model

In vivo binding ability of (^{18}F)BF-168 and (^{18}F)BF-227 to Aβ fibrils was further evaluated by the autoradiographic experiment in the Aβ-injected rat model. In an image of the brain section at 180 min postinjection of ^{18}F-labeled agents (Fig. 6), Aβ aggregates were clearly labeled with both agents, suggesting the usefulness of these agents as *in vivo* amyloid-imaging probes. However, non-specific

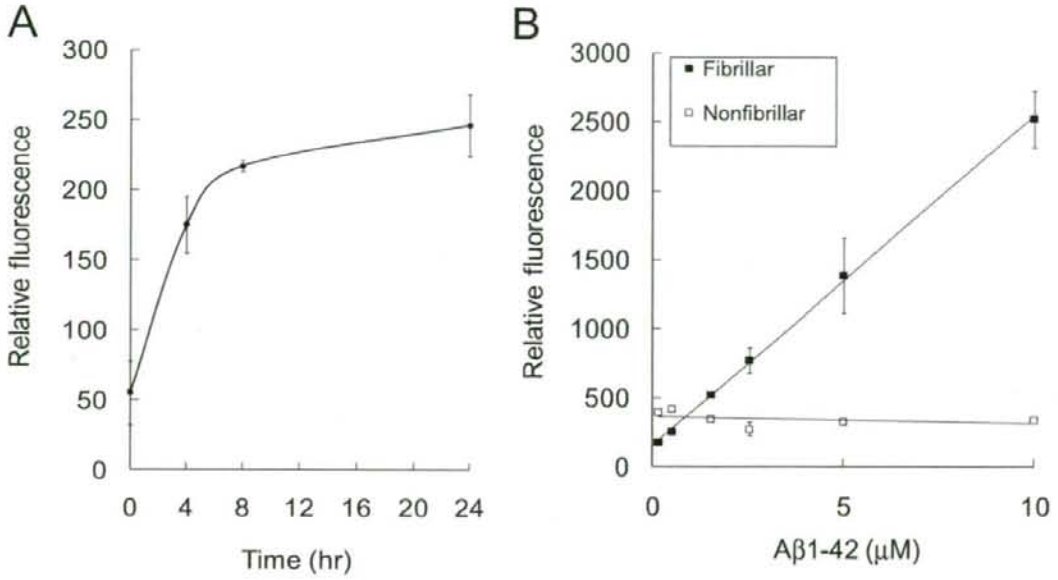

Figure 3 *In vitro* binding of BF-227 with Aβ peptides. Fluorescence intensity of BF-227 increased with Aβ incubation time (A). BF-227 fluorescence also increased linearly with concentrations of fibrillar Aβ, but did not increase in mixture with non-fibrillar Aβ (B).

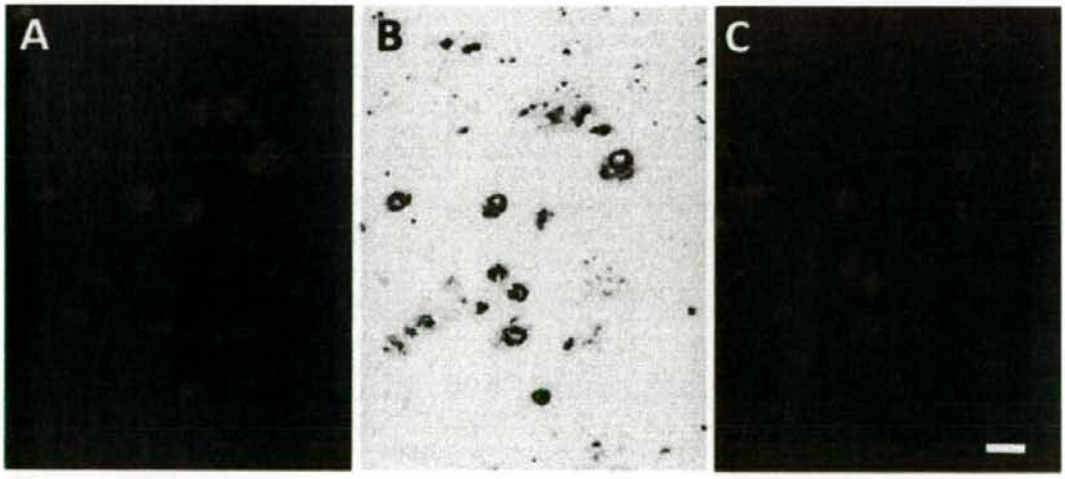

Figure 4 Neuropathological staining of Alzheimer's disease (AD) temporal brain sections by BF-227. Senile plaques are clearly stained with BF-227 (A). This staining correlates well with Aβ immunostaining in adjacent sections (B). BSB stains both senile plaques and neurofibrillary tangles (C). Bar, 200 μm.

retention of (^{18}F)BF-227 in the white matter was much less than that of (^{18}F)BF-168. This resulted in better hot spot-to-background contrast for (^{18}F)BF-227 (Fig. 6b) compared to (^{18}F)BF-168 (Fig. 6a).

Toxicity study of BF-227

In the acute toxicity study, i.v. administration of BF-227 in doses 0.1–10 mg/kg did not produce any significant

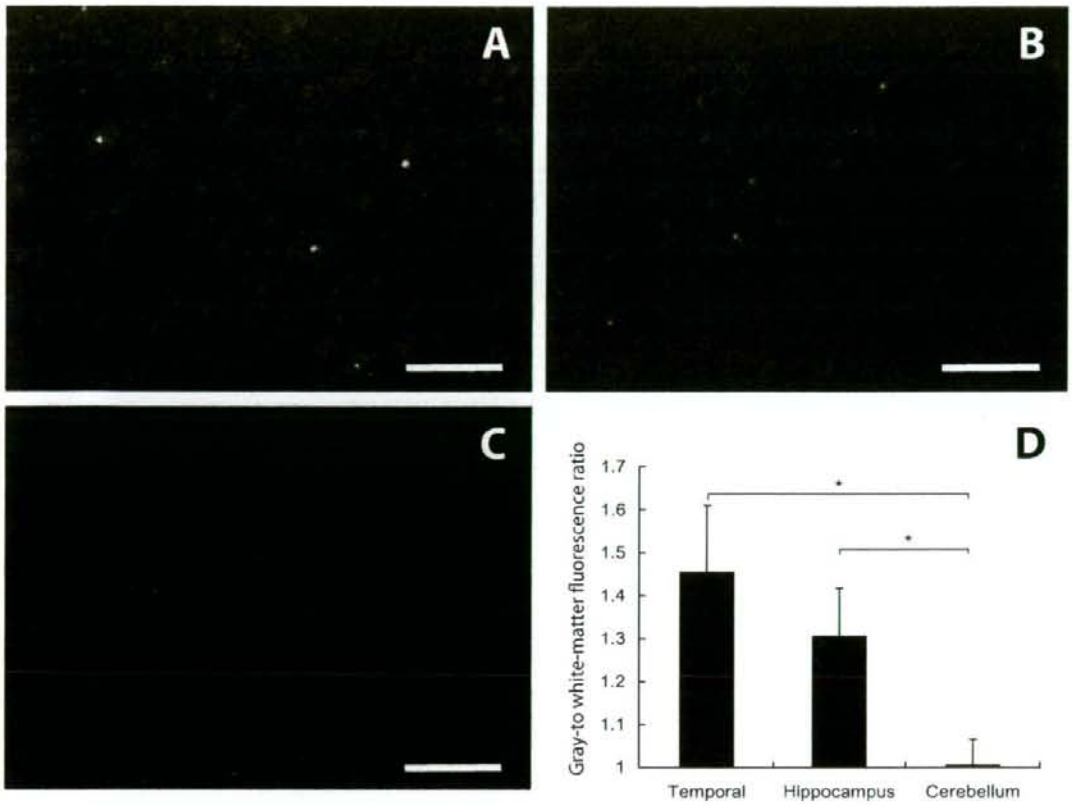

Figure 5 BF-227 staining in the temporal cortex (A), hippocampus (B) and cerebellum (C) of AD brain. In temporal and hippocampal brain sections, large numbers of amyloid plaques stained with BF-227. In contrast, no apparent staining was observed in the cerebellum. The stainability of BF-227 in the temporal cortex and hippocampus differed significantly from that in the cerebellum (D). $*P < 0.05$, one-way ANOVA followed by Scheffe's test.

changes in general behavior or bodyweight in male or female mice. During the 8 days of the experiment, no deaths occurred in any of the groups. This indicates that the dose for 50% lethality (LD_{50}) of i.v. administered BF-227 is higher than 10 mg/kg for male and female mice. In the subacute toxicity study, i.v. administration of BF-227 in tested doses did not produce any significant changes in general behavior or bodyweight in male or female mice. No significant differences in organ weight were observed between control and BF-227-administered groups. After the 14-day post-treatment period, mice did not show any microscopic alterations on pathological examination.

Discussion

Several research groups have worked to develop amyloid-imaging agents for use with PET. PIB is currently the most successful of these agents, showing high binding affinity for Aβ fibrils and fast clearance from normal brain tissue.[13] In the clinical trial, PIB-PET distinctly differentiated AD patients from normal individuals.[4] Other amyloid-imaging agents, such as SB-13,[14] IMPY[15] and benzofuran derivatives,[16] have also been explored for use as PET and single-photon emission computed tomography (SPECT) imaging probes. These agents display high binding affinity to Aβ fibrils. The key chemical structure common to these imaging agents is an aminophenyl group, which is considered essential for binding to the β-pleated sheet structure of Aβ fibrils. The present study, however, demonstrated that BF-227, a derivative of BF-168 with an aminothiazol group in place of the aminophenyl group, also binds strongly to amyloid-β fibrils. Furthermore, an autoradiographic study comparing BF-227 to BF-168 suggested that the aminothiazol group might contribute in a large way to

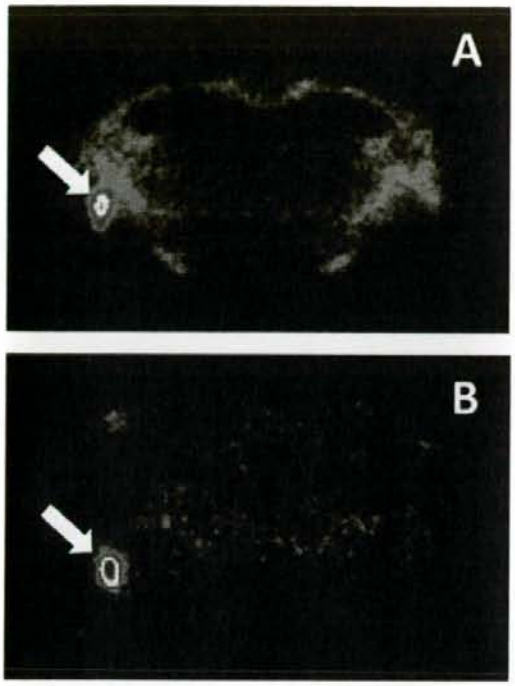

Figure 6 *In vivo* labeling of Aβ fibrils in brain sections from the Aβ-injected rat model with (^{18}F)BF-168 (A) and (^{18}F)BF-227 (B). Arrows indicate sites of Aβ injection.

decreased non-specific retention in normal brain tissue, particularly in white matter. This possibility should be examined in further studies, as this finding would be helpful in the design or modification of further series of amyloid-imaging agents.

Findings from the *in vitro* binding experiment indicated that the amount of BF-227 binding is proportional to the concentration of Aβ fibrils. Neuropathological findings also indicated that BF-227 preferentially binds to lesions containing dense Aβ fibrils. Densities of neuritic plaques are higher in the temporal, parietal and occipital lobes, moderate in the limbic lobe and lowest in the cerebellum.[17] Our results for BF-227 stainability in different brain regions were consistent with this neuropathological pattern of Aβ deposition in AD patients. Brains from patients with AD are characterized by an anatomically widespread process of amyloid deposition. Presence of neuritic or cored plaques is considered the best indication of the presence of the disease process underlying AD.[18] Quantitative measurement of Aβ fibril formation using BF-227 will thus allow discrimination of the disease process from normal aging processes. SP in the cerebellum are predominantly of the non-fibrillar type. The lack of obvious staining by BF-227 in the cerebellum thus suggests the binding preference of this compound to fibrillar Aβ.

The present study demonstrated high binding affinity of BF-227 to fibrillar Aβ and preferential binding to SP in AD brain sections. i.v. administration of this compound into an Aβ-injected rat model demonstrated selective binding to amyloid fibrils in the brain and faster clearance from white matter than BF-168. The toxicity study indicated that BF-227 is safe for clinical use as a PET probe, with a very wide margin between the lethal dose of BF-227 (>10 mg/kg) and clinical dose in human PET studies (<100 ng/kg). Considering all these findings together, BF-227 appears applicable for use as an *in vivo* amyloid-imaging agent. We are currently engaging in a clinical PET trial using ^{11}C-labeled BF-227 in AD patients.[19] This trial will elucidate the clinical utility of BF-227 in humans.

Acknowledgments

This study was partially supported by the Novartis Foundation for Gerontological Research, the Special Coordination Funds for Promoting Science and Technology, the Program for the Promotion of Fundamental Studies in Health Science by the National Institute of Biomedical Innovation, the Industrial Technology Research Grant Program from the New Energy and Industrial Technology Development Organization (NEDO) of Japan, Health and Labor Sciences Research Grants for Translational Research from the Japanese Ministry of Health, Labor and Welfare, a JST grant on research and education in molecular imaging, and an Astrazeneca Research Grant.

References

1 Price JL, Morris JC. Tangles and plaques in nondemented aging and "preclinical" Alzheimer's disease. *Ann Neurol* 1999; **45**: 358–368.
2 Nordberg A. PET imaging of amyloid in Alzheimer's disease. *Lancet Neurol* 2004; **3**: 519–527.
3 Klunk WE, Wang Y, Huang GF, Debnath ML, Holt DP, Mathis CA. Uncharged thioflavin-T derivatives bind to amyloid-beta protein with high affinity and readily enter the brain. *Life Sci* 2001; **69**: 1471–1484.
4 Klunk WE, Engler H, Nordberg A *et al.* Imaging brain amyloid in Alzheimer's disease with Pittsburgh Compound-B. *Ann Neurol* 2004; **55**: 306–319.
5 Agdeppa ED, Kepe V, Liu J *et al.* Binding characteristics of radiofluorinated 6-dialkylamino-2-naphthylethylidene derivatives as positron emission tomography imaging probes for beta-amyloid plaques in Alzheimer's disease. *J Neurosci* 2001; **21**: RC189.
6 Small GW, Kepe V, Ercoli LM *et al.* PET of brain amyloid and tau in mild cognitive impairment. *N Eng J Med* 2006; **355**: 2652–2663.
7 Okamura N, Suemoto T, Shimadzu H *et al.* Styrylbenzoxazole derivatives for in vivo imaging of amyloid plaques in the brain. *J Neurosci* 2004; **24**: 2535–2541.

8 Shimadzu H, Suemoto T, Suzuki M *et al.* Novel probes for imaging amyloid-β: F-18 and C-11 labeling of 2-(4-aminostyryl) benzoxazole derivatives. *J Label Compd Radiopharm* 2004; **47**: 181–190.
9 Okamura N, Suemoto T, Shiomitsu T *et al.* A novel imaging probe for in vivo detection of neuritic and diffuse amyloid plaques in the brain. *J Mol Neurosci* 2004; **24**: 247–255.
10 Suemoto T, Okamura N, Shiomitsu T *et al.* In vivo labeling of amyloid with BF-108. *Neurosci Res* 2004; **48**: 65–74.
11 Paxinos G, Watson C. *The Rat Brain in Stereotaxic Coordinates*. San Diego, CA: Academic Press, 1998.
12 Mathis CA, Klunk WE. Imaging β-amyloid plaques and neurofibrillary tangles in the aging human brain. *Curr Pharm Design* 2004; **10**: 1469–1492.
13 Mathis CA, Wang Y, Holt DP, Huang GF, Debnath ML, Klunk WE. Synthesis and evaluation of ^{11}C-labeled 6-substituted 2-arylbenzothiazoles as amyloid imaging agents. *J Med Chem* 2003; **46**: 2740–2754.
14 Verhoeff NP, Wilson AA, Takeshita S *et al.* In-vivo imaging of Alzheimer disease beta-amyloid with [^{11}C]SB-13 PET. *Am J Geriatr Psychiatry* 2004; **12**: 584–595.
15 Kung MP, Hou C, Zhuang ZP *et al.* Characterization of IMPY as a potential imaging agent for β-amyloid plaques in double transgenic PSAPP mice. *Eur J Nucl Med Mol Imaging* 2004; **31**: 1136–1145.
16 Ono M, Kawashima H, Nonaka A *et al.* Novel benzofuran derivatives for PET imaging of β-amyloid plaques in Alzheimer's disease brain. *J Med Chem* 2006; **49**: 2725–2730.
17 Arnold SE, Hyman BT, Flory J, Damasio AR, Van Hoesen GW. The topographical and neuroanatomical distribution of neurofibrillary tangles and neuritic plaques in the cerebral cortex of patients with Alzheimer's disease. *Cereb Cortex* 1991; **1**: 103–116.
18 Price JL. Diagnostic criteria for Alzheimer's disease. *Neurobiol Aging* 1997; **18**: S67–S70.
19 Kudo Y, Okamura N, Furumoto S *et al.* 2-[2-(2-dimethylaminothiazol-5-yl) ethenyl] -6-[2-(fluoro) ethoxy-]benzoxazole: a novel PET imaging agent for in vivo detection of dense amyloid plaques in Alzheimer's disease patients. *J Nucl Med* 2007; **48**: 553–561.

2-(2-[2-Dimethylaminothiazol-5-yl]Ethenyl)-6-(2-[Fluoro]Ethoxy)Benzoxazole: A Novel PET Agent for In Vivo Detection of Dense Amyloid Plaques in Alzheimer's Disease Patients

Yukitsuka Kudo[1], Nobuyuki Okamura[2], Shozo Furumoto[1], Manabu Tashiro[3], Katsutoshi Furukawa[4], Masahiro Maruyama[4], Masatoshi Itoh[3], Ren Iwata[5], Kazuhiko Yanai[2], and Hiroyuki Arai[4]

[1]Tohoku University Biomedical Engineering Research Organization (TUBERO), Sendai, Japan; [2]Department of Pharmacology, Tohoku University School of Medicine, Sendai, Japan; [3]Division of Cyclotron Nuclear Medicine, Cyclotron and Radioisotope Center, Tohoku University, Sendai, Japan; [4]Department of Geriatrics and Gerontology, Center for Asian Traditional Medicine, Tohoku University School of Medicine, Sendai, Japan; and [5]Division of Radiopharmaceutical Chemistry, Cyclotron and Radioisotope Center, Tohoku University, Sendai, Japan

Extensive deposition of dense amyloid fibrils is a characteristic neuropathologic hallmark in Alzheimer's disease (AD). Noninvasive detection of these molecules is potentially useful for early and precise detection of patients with AD. This study reports a novel compound, 2-(2-[2-dimethylaminothiazol-5-yl]ethenyl)-6-(2-[fluoro]ethoxy)benzoxazole (BF-227), for in vivo detection of dense amyloid deposits using PET. **Methods:** The binding affinity of BF-227 to amyloid-β (Aβ) fibrils was calculated. The binding property of BF-227 to amyloid plaques was evaluated by neuropathologic staining of AD brain sections. Brain uptake and in vivo binding of BF-227 to Aβ deposits were also evaluated using mice. For clinical evaluation of ^{11}C-BF-227 as a PET probe, 11 normal (healthy) subjects and 10 patients with AD participated in this study. Dynamic PET images were obtained for 60 min after administration of ^{11}C-BF-227. The regional standardized uptake value (SUV) and the ratio of regional to cerebellar SUV were calculated as an index of ^{11}C-BF-227 retention. The regional tracer distribution in AD patients was statistically compared with that of aged normal subjects on a voxel-by-voxel basis. **Results:** BF-227 displayed high binding affinity to synthetic Aβ1-42 fibrils (K_i [inhibition constant], 4.3 ± 1.5 nM). Neuropathologic staining has demonstrated preferential binding of this agent to dense amyloid deposits in AD brain. Moreover, a biodistribution study of this agent revealed excellent brain uptake and specific labeling of amyloid deposits in transgenic mice. The present clinical PET study using ^{11}C-BF-227 demonstrated the retention of this tracer in cerebral cortices of AD patients but not in those of normal subjects. All AD patients were clearly distinguishable from normal individuals using the temporal SUV ratio. Voxel-by-voxel analysis of PET images revealed that cortical BF-227 retention in AD patients is distributed primarily to the posterior association area of the brain and corresponded well with the preferred site for neuritic plaque depositions containing dense Aβ fibrils. **Conclusion:** These findings suggest that BF-227 is a promising PET probe for in vivo detection of dense amyloid deposits in AD patients.

J Nucl Med 2007; 48:553–561
DOI: 10.2967/jnumed.106.037556

Substantial neuropathologic evidence suggests that the deposition of senile plaques (SPs) and neurofibrillary tangles (NFTs) represents the characteristic neuropathologic hallmark in Alzheimer's disease (AD) (*1*). Progressive accumulation of SPs is considered fundamental to the initial development of dementia. Extensive deposition of SPs in the brain is present even in very mild AD and precedes the presentation of cognitive impairment (*2,3*). Several antiamyloid drugs are under development for the treatment and prevention of AD (*4*). For early detection and preventive intervention for AD, noninvasive imaging of neuropathologic lesions is a powerful strategy.

For this purpose, several imaging techniques have been developed that can noninvasively detect SPs in the brain using PET, SPECT, and MRI. Among these imaging modalities, PET is the most advanced and practical method for in vivo measurement of SP depositions. To achieve successful imaging using PET, various radiolabeled agents have been developed. Currently, 6OH-BTA-1 (PIB) is the most successful PET agent for in vivo amyloid imaging. This tracer sensitively detects amyloid fibrils in the brain and is proven to be useful for early diagnosis of AD (*5–7*).

However, amyloid-β (Aβ) deposition is also frequent in aging, even in cognitively intact individuals. Excessive identification of Aβ has a potential risk to misjudge the normal aging process with abnormal Aβ deposition. In the

Received Oct. 23, 2006; revision accepted Jan. 20, 2007.
For correspondence or reprints contact: Nobuyuki Okamura, MD, Department of Pharmacology, Tohoku University School of Medicine, 2-1, Seiryo-machi, Aoba-ku, Sendai 980-8575, Japan.
E-mail: oka@mail.tains.tohoku.ac.jp

normal aging process, noncompact or diffuse amyloid plaques containing less fibrillar Aβ are deposited primarily in the brain. Brains from patients with AD are characterized by an anatomically widespread process of amyloid deposition and neuritic plaque formation containing dense amyloid fibrils (*8*). A shift of brain Aβ from the soluble to the fibrillar form is closely associated with the onset of AD (*9*). Therefore, selective detection of dense amyloid fibrils would be advantageous to differentiate the normal aging process from AD with high specificity.

We have previously demonstrated a novel series of benzoxazole derivatives as promising candidates for an in vivo imaging probe of SPs (*10–12*). These derivatives showed comparatively high blood–brain barrier (BBB) permeability, high binding affinity for Aβ aggregates, and high specificity for fibrillar Aβ deposits, suggesting potential merit for the early detection of AD-related pathologies. Herein we introduce an optimized derivative, 2-(2-[2-dimethylaminothiazol-5-yl]ethenyl)-6-(2-[fluoro]ethoxy)benzoxazole (BF-227), as a PET probe for in vivo detection of dense amyloid deposits in humans.

MATERIALS AND METHODS

Preparation of Compounds

BF-227 (Fig. 1) and its *N*-desmethylated derivative (a precursor of ^{11}C-BF-227) were custom-synthesized by Tanabe R&D Service Co. ^{11}C-BF-227 was synthesized from the precursor by *N*-methylation in dimethyl sulfoxide (Fig. 1) using ^{11}C-methyl triflate (*13,14*). After quenching the reaction with 5% acetic acid in ethanol, ^{11}C-BF-227 was separated from the crude mixture by semipreparative reversed-phase high-performance liquid chromatography and then isolated from the collected fraction by solid-phase extraction. The purified ^{11}C-BF-227 was solubilized in isotonic saline containing 1% polysobate-80 and 5% ascorbic acid. The saline solution was filter-sterilized with a 0.22-μm Millipore filter for clinical use. The radiochemical yields were >50% based on ^{11}C-methyl triflate, and the specific radioactivities were 119–138 GBq/μmol at the end of synthesis. The radiochemical purities were >95%.

In Vitro Binding Assays

Binding affinities of the compounds for synthetic Aβ1-42 aggregates were examined as described previously (*10*). Briefly, solid-form Aβ1-42 (Peptide Institute) was dissolved in 10 mM potassium phosphate buffer (pH 7.4) and incubated at 37°C for 40 h. The binding assay was performed by mixing 100 μL of aggregated Aβ1-42 with the appropriate concentration of ^{125}I-labeled 2-(4-methylamino)styryl-5-iodo-benzoxazole (BF-180) and 8% ethanol. After incubation for 4 h at room temperature, the binding mixture was filtered and filters containing bound ^{125}I ligand were counted using a γ-counter. The dissociation constant (K_d) and maximum specific binding (B_{max}) of BF-180 were determined. For inhibition studies, binding studies were performed using synthetic Aβ1-42 aggregates. A mixture containing 50 μL of BF-227, 50 μL of 0.05 nM ^{125}I-BF-180, 100 μL of 100 nM Aβ1–42, and 800 μL of 8% ethanol was incubated at room temperature for 4 h. The mixture was then filtered through Whatman GF/B filters, and filters containing bound ^{125}I ligand were counted in a γ-counter. Values for the half-maximal inhibitory concentration (IC_{50}) were determined from displacement curves of 3 independent experiments using Prism software (GraphPad), and values for the inhibition constant (K_i) were determined using the Cheng–Prusoff equation.

Measurement of Octanol/Water Partition Coefficients

Phosphate-buffered saline (PBS) and 1-octanol (Wako) were saturated with 1-octanol and PBS, respectively, before use. BF-227 was dissolved in 1-octanol and shaken with equal amounts of PBS for 30 min at room temperature. After centrifugation at 2,000 rpm for 15 min, absorbency of the 1-octanol layer was measured at the peak wavelength of the absorbance spectrum of BF-227 using a Spectra Max 190 microplate reader (Molecular Devices). Octanol/water partition coefficients were determined by comparing absorbency with that before shaking with PBS. Each data point was performed in duplicate.

BBB Permeability of BF-227 in Normal Mice

Brain uptake of BF-227 was measured using ^{11}C-labeled compound. The ^{11}C-BF-227 (1.1–6.3 MBq) was administered into the tail vein of male C57B6 mice (n = 23; mean weight, 28–32 g). Mice were then sacrificed by decapitation at 2, 10, 30, and 60 min after injection. The whole brain was removed and weighed, and radioactivity was counted using an automatic γ-counter. The percentage injected dose per gram of tissue (%ID/g) was calculated by normalizing tissue counts to tissue weight. Each %ID/g value is expressed as a mean ± SD of 3 or 4 separate experiments.

Neuropathologic Staining

Postmortem brain tissues from a 69-y-old man with autopsy-confirmed AD and an 81-y-old man with autopsy-confirmed physiologic aging were obtained from Fukushimura Hospital (Toyohashi, Japan). Experiments were performed under the regulations of the ethics committee of BF Research Institute. Serial sections (6-μm thick) from paraffin-embedded blocks of temporal cortex, striatum, and cerebellum were prepared in xylene and ethanol. Before

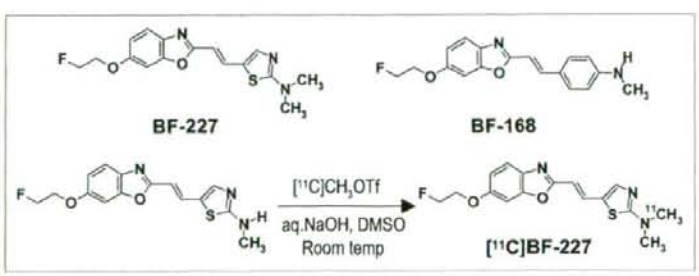

FIGURE 1. Chemical structures of BF-227 and BF-168 and radiosynthesis of BF-227.

the staining of compounds, quenching of autofluorescence was performed as described previously. Quenched tissue sections were immersed in 100 μM of BF-227 or 0.125% thioflavin-S solution containing 50% ethanol for 10 min. Sections stained with each compound were then dipped briefly into water and rinsed in PBS for 60 min before coverslipping with Fluor Save Reagent (Calbiochem); sections were examined using an Eclipse E800 microscope (Nikon) equipped with a V-2A filter set (excitation, 380–420 nm; dichroic mirror, 430 nm; long-pass filter, 450 nm). Sections stained with thioflavin-S were dipped briefly in tap water and in 50% ethanol and then washed in PBS for 60 min before coverslipping; this was followed by fluorescent microscopy using a BV-2A filter set (excitation, 400–440 nm; dichroic mirror, 455 nm; long-pass filter, 470 nm). In addition, adjacent sections were immunostained using monoclonal antibody (mAb) against Aβ (6F/3D; Dako A/S). After pretreatment with 90% formic acid for 5 min, sections were immersed in blocking solution for 30 min and then incubated for 60 min at 37°C with 6F/3D at a dilution of 1:50. After incubation, sections were processed by the avidin–biotin method using a Pathostain ABC-POD(M) Kit (Wako) and diaminobenzidine tetrahydrochloride.

Labeling of Aβ Deposits in Transgenic Mouse Brain

Ex vivo plaque labeling with BF-227 was evaluated using PS1/APPsw double transgenic mice (n = 2) and a wild-type mouse (n = 1) (male, 32-wk old) (*15*). A BF-227 solution containing 10% polyethylenglycol 400 and 0.1 mol/L HCl was administered into the tail vein at a dose of 4 mg/kg. Mice were anesthetized using sodium pentobarbital 2 h after injection of BF-227; they were then perfused transcardially with ice-cold saline, which was followed by 4% paraformaldehyde in 0.1 M PBS, and the brains were removed. After cryoprotection in 30% sucrose/0.1 M PBS, 6-μm frozen sections were cut using an OTF cryostat and imaged with no additional staining for fluorescent microscopy using a V-2A filter set. The same sections were immunostained using mAb against Aβ (6F/3D) as described earlier.

Subjects and Patients in Clinical PET Study

Eleven normal (healthy) control subjects, including 3 young normal subjects and 8 aged-matched normal subjects, and 10 probable AD patients underwent PET measurement of ^{11}C-BF-227 distribution in the brain (Table 1). AD patients were recruited through the Tohoku University Hospital Dementia Patients Registry. The diagnosis of AD was made according to the National Institute of Neurological and Communicative Diseases and Stroke/Alzheimer's Disease and Related Disorders Association (NINCDS–ADRDA) criteria. The normal control group was recruited from volunteers, who were taking no centrally acting medication, had no cognitive impairment, and had no cerebrovascular lesion on MR images. No significant difference in age was apparent between the AD group and the aged normal control group. AD patients had significantly lower mean mini-mental status examination (MMSE) scores than normal control subjects. This study was approved by the ethics committee on clinical investigations of Tohoku University School of Medicine and was performed in accordance with the Declaration of Helsinki. After complete description of the study to the patients and subjects, written informed consent was obtained.

Image Acquisition Protocols

The protocol of the PET study was approved by the Committee on Clinical Investigation at The Tohoku University School of Medicine and the Advisory Committee on Radioactive Substances at Tohoku University. The ^{11}C-BF-227 PET study was performed using a SET-2400W PET scanner (Shimadzu). After intravenous injection of 211–366 MBq of ^{11}C-BF-227, dynamic PET images were obtained for 60 min (23 sequential scans: 5 scans × 30 s, 5 scans × 60 s, 5 scans × 150 s, and 8 scans × 300 s) with each subject's eyes closed. The T1-weighted MR images were obtained using a SIGNA 1.5-T machine (GE Healthcare).

TABLE 1
Subject Demographics

Group	Subject	Sex	Age (y)	MMSE score
Young normal (n = 3)	YN 1	M	36	30
	YN 2	M	37	30
	YN 3	M	36	30
	Mean ± SD		36.3 ± 0.6	30.0 ± 0.0
Aged normal (n = 8)	AN 1	M	69	30
	AN 2	F	70	29
	AN 3	F	64	30
	AN 4	F	65	30
	AN 5	M	67	30
	AN 6	M	69	30
	AN 7	M	71	30
	AN 8	M	59	30
	Mean ± SD		66.8 ± 4.0	29.9 ± 0.4
All normal (n = 11)	Mean ± SD		58.5 ± 14.6	29.9 ± 0.3
AD (n = 10)	AD 1	F	65	24
	AD 2	M	75	19
	AD 3	F	72	21
	AD 4	F	82	18
	AD 5	F	62	20
	AD 6	F	68	21
	AD 7	M	70	23
	AD 8	F	85	23
	AD 9	M	78	14
	AD 10	F	75	26
	Mean ± SD		73.2 ± 7.3*	20.9 ± 3.4*†

*P < 0.05 vs. young normal group.
†P < 0.05 vs. aged normal group.
MMSE = mini-mental state examination.

Image Analysis

First, standardized uptake value (SUV) images of ^{11}C-BF-227 were obtained by normalizing tissue radioactivity concentration by injected dose and body weight. Subsequently, individual MR images were anatomically coregistered into individual PET images using Statistical Parametric Mapping software (SPM2; Wellcome Department, U.K.) (*16*). Regions of interest (ROIs) were placed on individual axial MR images in the cerebellar hemisphere, striatum, thalamus, frontal cortex (Brodmann's areas [BA] 8, 9, 10, 44, 45, 46, and 47), lateral temporal cortex (BA 21, 22, 37, and 38), parietal cortex (BA 39 and 40), temporooccipital cortex (BA 18 and 19), occipital cortex (BA 17), medial temporal cortex (BA 27, 28, 34, and 35), pons, and subcortical white matter, as described previously (*17*). The ROI information was then copied onto dynamic PET SUV images, and regional SUVs were sampled using Dr.View/LINUX software (Asahi-Kasei Joho System).

The interrater reliability for the ROI measurement was tested between 2 raters in 14 subjects and patients. The intraclass correlation coefficient was 0.95 in the frontal cortex and cerebellum, 0.97 in the lateral temporal and parietal cortices, and 0.98 in the medial temporal cortex. The correlation coefficient between these 2 measurements was 0.96 in the frontal cortex, 0.97 in the lateral temporal cortex, and 0.99 in the parietal cortex, medial temporal cortex, and cerebellum. SUVs between 40 and 60 min were averaged to calculate the SUVs for group comparison.

Statistical Analysis

For statistical comparison in the 3 groups, we applied the Kruskal–Wallis test, which was followed by Dunn's multiple comparison test. The difference in time–activity curves in ^{11}C-BF-227 PET was also evaluated by repeated measures ANOVA, which was followed by the Bonferroni–Dunn post hoc test. For statistical comparisons of PET measurements in aged normal and AD groups, we used the Mann–Whitney U test. Effect-size coefficients (Cohen's d) were also calculated for the evaluation of group differences in PET measurements. Statistical significance for each analysis was defined as $P < 0.05$. Statistical comparison between images from normal control subjects and AD patients was performed on a voxel-by-voxel basis using SPM2 software (*16*). SUV summation images 30–60 min after injection were stereotactically normalized using individual MR images into a standard space of Talairach and Tournoux. The normalized images were smoothed using a $16 \times 16 \times 16$ mm gaussian filter. The count of each voxel was normalized to the cerebellar ROI value, because cerebellum is reported to be a region free of fibrillar amyloid plaques in AD brain. Images of patients with AD ($n = 10$) were compared with those of aged normal control subjects ($n = 8$) for between-group analysis ($P < 0.001$, uncorrected; extent threshold, $k = 200$). For the group analysis, a 2-sample t test was used to detect differences between the AD and normal control groups.

RESULTS

In Vitro Binding Study for Aβ Fibrils

In vitro binding assay indicated that BF-227 shows high binding affinity for Aβ1-42 fibrils. K_i for Aβ1-42 fibrils in competitive binding assay using ^{125}I-BF-180 was 4.3 ± 1.5 nM in BF-227, comparable to levels previously reported for compound BF-168.

Neuropathologic Staining in AD Brain Sections

Neuropathologic examination using BF-227 indicated that amyloid plaques were selectively stained with BF-227 in AD brain sections (Fig. 2A). Especially, cored plaques were brightly stained with BF-227, indicating that this compound preferentially binds to mature amyloid plaque. This staining pattern correlated well with Aβ immunostaining in adjacent sections (Fig. 2B, arrows). BF-227 staining was further compared with staining using thioflavin-S. In contrast to clear staining of SPs and NFTs with thioflavin-S (Fig. 2C), BF-227 primarily stained SPs, with faint staining of NFTs (Fig. 2B, arrowheads). No apparent staining was also observed in the temporal brain section of the aged normal case (Fig. 2D).

BBB Permeability and Clearance from Normal Brain

Next, we investigated whether BF-227 entered the brain in amounts sufficient for use as a PET agent. The log P value of BF-227 was 1.75, close to that of BF-168 (log P = 1.79). Intravenous administration of BF-227 into normal mice indicated that this compound readily penetrated the BBB. Brain uptakes at 2, 10, 30, and 60 min after intravenous injection of ^{11}C-BF-227 were 7.9 ± 1.3, 3.7 ± 0.37, 1.4 ± 0.36, and 0.64 ± 0.15 %ID/g, respectively. ^{11}C-BF-227 displayed double the initial uptake and faster washout

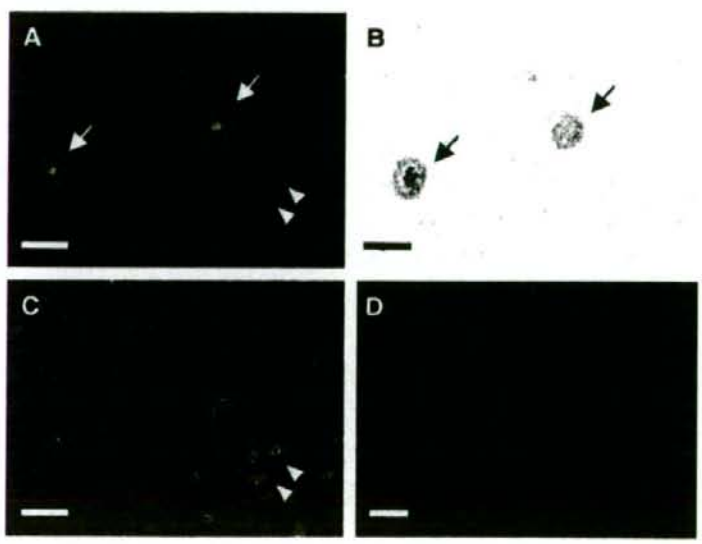

FIGURE 2. Neuropathologic staining of human brain sections by BF-227. Amyloid plaques are clearly stained with BF-227 in AD temporal brain sections (A). BF-227 staining correlates well with Aβ immunostaining in adjacent sections (B, arrows). BF-227 faintly stains NFTs, in contrast to clear staining with thioflavin-S (C, arrowheads). In aged normal temporal cortex (D), no staining by BF-227 is observed. Bar in A–C = 50 μm; bar in D = 200 μm.

in normal brain tissue compared with those of ^{18}F-BF-168 (3.9 %ID/g at 2 min after injection; 1.3 %ID/g at 60 min after injection).

Intravenous Administration of BF-227 in Transgenic Mice

In vivo binding of nonlabeled BF-227 to Aβ deposits was examined using PS1/APPsw double transgenic mice. After intravenous injection of 4 mg/kg BF-227, ex vivo observation of transgenic mouse brain slices showed numerous fluorescent spots in the neocortex and hippocampus (Figs. 3A and 3B). In contrast, no fluorescent spots were detected in the wild-type mouse brain (Fig. 3C). Brain sections of transgenic mice were subsequently immunostained using Aβ-specific antibody, and the distribution of plaques labeled with BF-227 corresponded well with Aβ immunostaining (Fig. 3D, arrowheads).

Time–Activity Data of ^{11}C-BF-227 in Clinical PET Study

No toxic event was observed in the current clinical trial of ^{11}C-BF-227. The SUV time–activity curves from ^{11}C-BF-227 PET in AD patients and all normal subjects are shown in Figure 4. Both groups showed rapid entry of ^{11}C-BF-227 into gray matter areas. In AD patients, the frontal, temporal, and parietal cortices, areas known to contain high concentrations of fibrillar amyloid plaques in AD, retained ^{11}C-BF-227 to a greater extent during the later time points compared with normal subjects (Figs. 4A–4C). When the 2 groups were compared, a significant difference in time–activity curves was observed in the frontal (Fig. 4A), lateral temporal (Fig. 4B), parietal (Fig. 4C), and visual association cortices (data not shown). In contrast, time–activity curves in the cerebellum (Fig. 4D), an area lacking fibrillar amyloid plaques, were nearly identical in normal subjects and AD patients. The subcortical white matter region showed relatively lower entry and slower clearance than gray matter areas but no significant difference in time–activity curves between the 2 groups (data not shown). In the comparison of time–activity curves in the cortical areas and cerebellum, AD patients showed a significant difference in time–activity curves over 10 min after administration of ^{11}C-BF-227, but normal subjects showed no significant differences.

SUV Images in AD Patients and Normal Control Subjects

SUV images summed over 20−40 min after injection of an aged normal subject (70-y-old woman) and an AD patient (68-y-old woman; MMSE score = 21) are shown in Figure 5. Cortical retention of ^{11}C-BF-227, especially in the basal portion of the frontal, temporal, and parietal region, was evident in the AD patient, in contrast with the images of the aged normal subject. This pattern of distribution is consistent with the findings of neuritic plaque distribution in postmortem AD brains (*18*). Higher retention of ^{11}C-BF-227 was also observed in the brainstem and thalamus; however, similar retention in these areas was detected in the aged normal subject. ^{11}C-BF-227 uptake in the cerebellum was relatively sparse in both the aged normal subject and the AD patient.

Comparisons of Regional SUVs and SUV Ratios

In the quantitative comparison of regional SUVs between 40 and 60 min after administration, cortical regions showed the tendency to be increased in AD patients; however, the difference was not significant because of the large individual difference in SUVs. SUVs in the thalamus, pons, and white matter were similar in the 3 groups. Because there were no plaques in the cerebellum, there was no BF-227 binding and no significant difference in the SUV between AD and normal groups, indicating that the cerebellum is adequate as a reference region. Therefore, the ratio of regional SUV to cerebellar SUV (SUV ratio) was calculated as an index of ^{11}C-BF-227 retention. This analysis successfully reduced the intersubject variability, as reflected in low SD values (Table 2). The mean SUV ratio for the frontal, lateral temporal, parietal, temporooccipital, occipital, anterior and posterior cingulate cortices, and striatum was significantly greater in AD patients than that in aged normal subjects (Table 2; Fig. 6). Notably, the SUV ratio in the lateral temporal cortex showed no overlap between AD patients and normal control subjects (Fig. 6). The SUV ratio in the medial temporal cortex, thalamus,

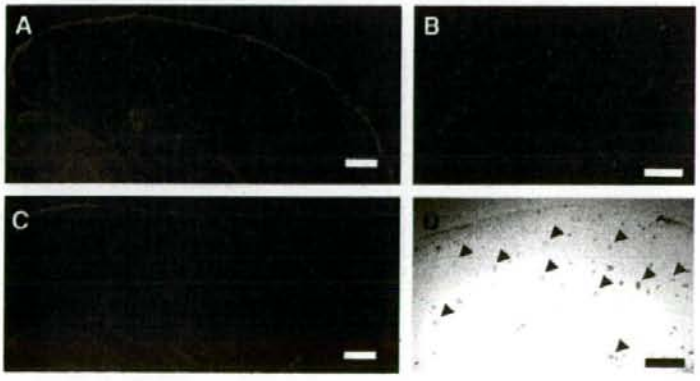

FIGURE 3. In vivo binding of BF-227 to amyloid plaques in PS1/APP transgenic mouse. In brain sections from PS1/APP transgenic mouse after intravenous injection of 4 mg/kg BF-227, numerous fluorescent spots were observed in neocortex and hippocampus of brain (A and B). In contrast, no fluorescent spots were observed in brain of wild-type mouse (C). Distribution of plaques labeled with BF-227 corresponded well with Aβ immunostaining in same section (B and D, arrowheads).

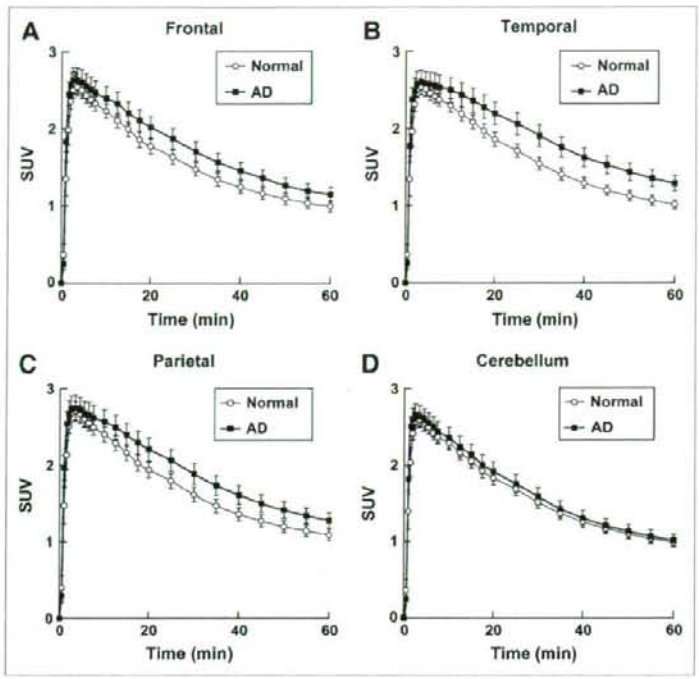

FIGURE 4. Time–activity data for ^{11}C-BF-227 PET in humans. SUV time–activity curves of ^{11}C-BF-227 in frontal cortex (A), temporal cortex (B), parietal cortex (C), and cerebellum (D) are shown. Each point represents mean ± SEM of data from 7 AD patients and 7 normal control subjects.

pons, and white matter was nearly identical in AD patients and normal subjects. The effect size between AD patients and aged normal subjects was highest in the lateral temporal cortex, which was followed by the parietal, anterior cingulate, and frontal cortices, and was lowest in the medial temporal, thalamus, and pons (Table 2). No significant difference was observed in any brain regions between young normal and aged normal subjects, although aged individuals tended to exhibit a higher SUV ratio in the frontal cortex than young individuals (data not shown).

Voxel-by-Voxel Analysis of ^{11}C-BF-227 PET Images

In comparison with aged normal subjects, AD patients showed significantly higher uptake of ^{11}C-BF-227 in the bilateral temporoparietal region ([50, −56, 6], Z = 5.41, k = 22,823), including the posterior cingulate cortex and the left middle frontal gyrus ([−26, 24, 40], Z = 3.79, k = 1,401) in SPM analysis (Fig. 7). These areas corresponded well with the region containing a high density of neuritic plaques. In contrast, no significant region was detected showing lower uptake of ^{11}C-BF-227 in the AD group than that in the normal group.

DISCUSSION

BF-227 was designed to improve BBB penetration and clearance from normal brain tissue, without deteriorating the high binding affinity of benzoxazole derivatives to Aβ. Several lipophilic compounds have been reported as potential amyloid imaging probes. 2-(1-{6-[(2-Fluoroethyl)(methyl) amino]-2-naphthyl}ethylidene)malononitrile (FDDNP) was introduced as the first BBB-permeable compound for in

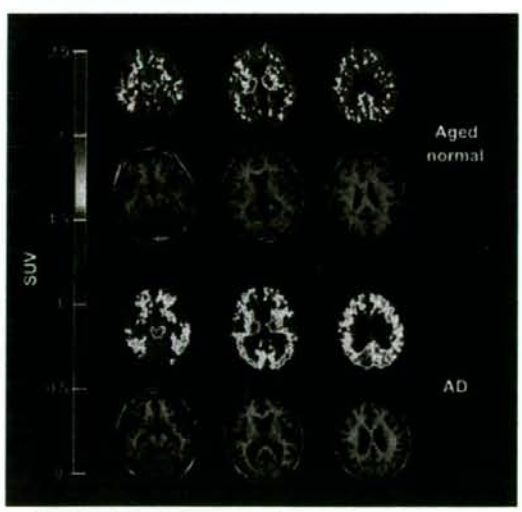

FIGURE 5. Mean SUV images between 20 and 40 min after injection of ^{11}C-BF-227 in aged normal subject (top, 70-y-old woman) and AD patient (bottom, 68-y-old woman). Coregistered MR images are shown below PET images.

TABLE 2
Regional SUV and Regional-to-Cerebellar SUV Ratio of ^{11}C-BF-227 in Normal Subjects and AD Patients

Distribution	SUV			SUV ratio			Cohen's *d*, Aged normal vs. AD
	All normal	Aged normal	AD	All normal	Aged normal	AD	
Frontal	1.13 ± 0.23	1.11 ± 0.24	1.24 ± 0.27	0.99 ± 0.04	0.99 ± 0.05	1.13 ± 0.06*	2.54
Lateral temporal	1.16 ± 0.22	1.15 ± 0.23	1.38 ± 0.30	1.03 ± 0.05	1.02 ± 0.04	1.25 ± 0.06*	4.51
Parietal	1.22 ± 0.24	1.19 ± 0.24	1.36 ± 0.30	1.08 ± 0.06	1.06 ± 0.05	1.24 ± 0.06*	3.26
Temporooccipital	1.22 ± 0.23	1.21 ± 0.24	1.35 ± 0.27	1.08 ± 0.06	1.08 ± 0.06	1.23 ± 0.09*	1.96
Occipital	1.23 ± 0.23	1.21 ± 0.24	1.32 ± 0.26	1.09 ± 0.06	1.08 ± 0.06	1.20 ± 0.07*	1.84
Anterior cingulate	1.19 ± 0.26	1.16 ± 0.26	1.27 ± 0.26	1.04 ± 0.04	1.03 ± 0.04	1.16 ± 0.06*	2.55
Posterior cingulate	1.28 ± 0.25	1.24 ± 0.25	1.38 ± 0.26	1.13 ± 0.08	1.11 ± 0.08	1.26 ± 0.04*	2.37
Medial temporal	1.33 ± 0.24	1.31 ± 0.25	1.31 ± 0.27	1.18 ± 0.07	1.17 ± 0.07	1.20 ± 0.10	0.35
Striatum	1.57 ± 0.34	1.52 ± 0.34	1.62 ± 0.34	1.38 ± 0.08	1.35 ± 0.06	1.47 ± 0.06*	2.00
Thalamus	1.78 ± 0.44	1.70 ± 0.41	1.73 ± 0.36	1.56 ± 0.12	1.51 ± 0.09	1.58 ± 0.11	0.70
Pons	1.90 ± 0.34	1.87 ± 0.34	1.91 ± 0.39	1.68 ± 0.08	1.67 ± 0.08	1.74 ± 0.09	0.82
White matter	1.64 ± 0.27	1.61 ± 0.28	1.69 ± 0.33	1.45 ± 0.11	1.44 ± 0.11	1.55 ± 0.12	0.96
Cerebellum	1.14 ± 0.23	1.13 ± 0.24	1.10 ± 0.23				

*$P < 0.05$ vs. aged normal group.

vivo imaging of amyloid. FDDNP specifically binds to both SPs and NFTs in AD brain sections (*19*). After intravenous injection of FDDNP, greater accumulation was observed in SP- and NFT-rich areas of the human brain (*20*). Thioflavin-T derivatives without any positive charge also show high permeability of the BBB. One of these compounds, PIB, was applied in a human PET study and enabled successful differentiation between AD patients and healthy normal individuals (*5*). Another amyloid-imaging agent, SB-13, was also applied in a human PET study and exhibited binding properties similar to those of PIB (*21*). Several iodinated agents, 6-iodo-2-(4′-dimethylamino-) phenyl-imidazo[1,2-*a*]-pyridine (IMPY) and I-stilbene, have also been explored for use as SPECT probes (*22*). Although validation remains necessary to determine whether retention of these agents in the neocortex truly reflects the level of amyloid deposition, such findings suggest the potential usefulness of this technique for early diagnosis of AD.

The results of the in vitro binding experiment indicate that binding of BF-227 reflects the amount of Aβ fibril deposition. In neuropathologic staining of AD brain sections, the fluorescence intensity of BF-227 is highest in the core region of mature amyloid deposits, which contain dense fibrils of Aβ. Conversely, diffuse plaques containing fewer Aβ fibrils are faintly stained by BF-227. SPs in the cerebellum are predominantly of the nonfibrillar type (*23,24*), and BF-227 only faintly stained diffuse amyloid plaques in the cerebellum. Thus, the absence of ^{11}C-BF-227 accumulation in the cerebellum of AD patients suggests the binding preference of this compound for fibrillar Aβ. This finding also indicates that the cerebellum is suitable as a reference region in the quantitative analysis of ^{11}C-BF-227 PET data.

PIB is currently the most successful of several amyloid-imaging agents. A clinical PET study in AD patients showed higher uptake of PIB in cortical areas and striatum, particularly the frontal and parietal cortices (*5–7*). In contrast, the current study demonstrated higher cortical retention of ^{11}C-BF-227 in the temporoparietal–occipital region rather than that in the frontal cortex and the striatum in AD patients. Both agents are considered to preferentially bind to the β-sheet structure of Aβ fibrils. What other factors could

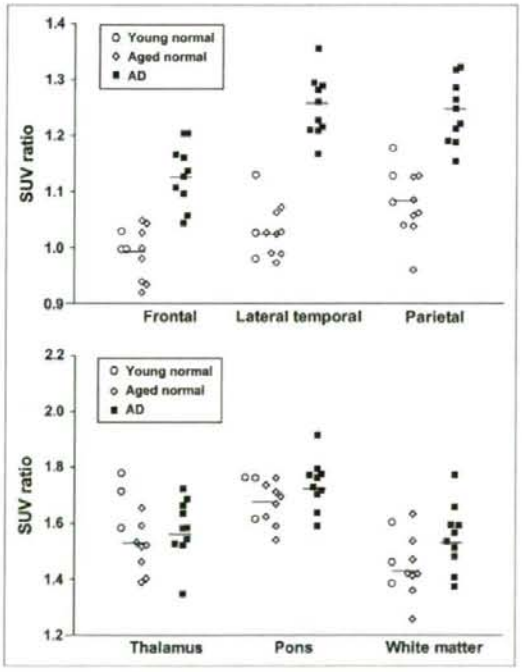

FIGURE 6. ROI/cerebellar SUV ratio in young normal subjects (○), aged normal subjects (◇), and AD patients (■). Vertical bar represents average SUV ratio in all normal subjects ($n = 11$) and AD patients ($n = 10$).

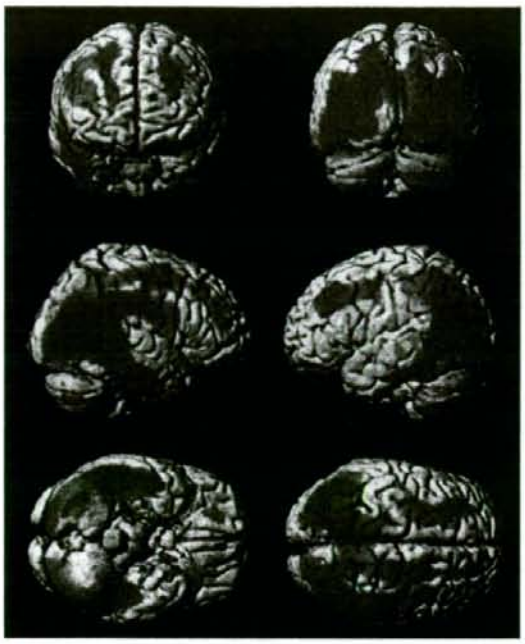

FIGURE 7. Brain regions show significantly elevated SUVs in AD patients compared with data from aged healthy subjects ($P < 0.001$, uncorrected for multiple comparisons).

have caused the difference of tracer distribution between previous PIB studies and the current BF-227 study? Generally, substantial individual variations exist in the amount and spatial distribution of amyloid deposition in AD. Thus, the discrepancy might be partially attributable to a difference in sample populations between studies. To settle this issue, a direct comparison study between PIB and BF-227 should be conducted using the same sample populations. SP is a heterogeneous class of protein aggregates with a β-pleated structure. Compact plaques consist of a dense central core of amyloid fibrils, and noncompact plaques contain less fibrillar Aβ (*25*). Therefore, it would be expected that the lower-affinity compound would tend to detect only SPs with dense Aβ fibrils and that the higher-affinity compound could bind SPs with both dense and moderately fibrillar Aβ. In AD patients, the difference between cortical and cerebellar SUV in ^{11}C-BF-227 PET was less than that in PIB PET (*5–7*), suggesting that the in vivo binding affinity of BF-227 to Aβ deposits is relatively lower than that of PIB. If so, BF-227 binds more preferentially to dense amyloid deposits than PIB. Previous neuropathologic studies have indicated that neuritic plaque densities are highest in the neocortex, especially the temporoparieto–occipital region, and lowest in the cerebellum (*18,26*). Data from SPM analysis are consistent with the postmortem distribution of neuritic plaque deposition in AD patients. Therefore, the difference in cortical distribution between BF-227 and PIB might be due to the difference in binding affinity to Aβ fibrils. A PET probe binding selectively to neuritic plaques would be less subject to Aβ pathology in the normal aging process. Thus, use of ^{11}C-BF-227 PET will allow accurate diagnosis of AD and might reduce false-positive findings in normal individuals. ^{11}C-BF-227 PET might also be useful for tracking the progression of fibrillar Aβ deposition in AD patients. Longitudinal PET investigation of AD patients will elucidate the utility of this imaging technique for monitoring disease progression in AD.

NFTs stained faintly with BF-227, suggesting that BF-227 has a relatively lower binding affinity to NFTs than SPs, which might explain the lack of significant difference in the medial temporal SUV of ^{11}C-BF-227. However, 3 AD patients (AD 1, AD 2, and AD 3 in Table 1) exhibiting high BF-227 accumulation in the cerebral cortex showed higher accumulation in the medial temporal cortex than the other AD patients. This finding might reflect the increasing deposition of amyloid plaques in the medial temporal cortex of the 3 AD patients. Thalamic and white matter accumulation of ^{11}C-BF-227 was considerable in both AD patients and normal subjects. Retention levels of ^{11}C-BF-227 in these regions were nearly identical between normal and AD groups. Therefore, these retentions are not likely to reflect AD-specific pathology. BF-227 retention in these sites may be related to the many myelinated fibers present in these structures, because myelin basic protein—one of the major myelin proteins in the brain—partially shares the same structure with amyloid fibrils, and some β-sheet binding agents bind to this protein (*27–29*). Clearance of ^{11}C-BF-227 from normal brain tissue was slower than that of PIB. This might be caused by the difference in lipophilicity between BF-227 and PIB. BF-227 (log $P = 1.75$) is more lipophilic than PIB (log $P = 1.20$) (*30*) because, unlike PIB, BF-227 does not have a hydroxy group. Compounds that are too lipophilic will be bound by plasma protein and undergo rapid metabolism by the liver; therefore, they may display reduced brain uptake. Moreover, lipophilic radioligands display a higher nonspecific binding in the brain and, thus, high nonspecific binding may explain the moderate difference in BF-227 uptake between AD patients and normal control subjects. In general, the introduction of a hydroxy group into a molecule changes the partition coefficient toward more hydrophilicity. Therefore, the hydroxylated BF-227 derivative would be expected to show faster clearance from normal brain tissue and a better signal-to-noise ratio than BF-227. We are now implementing the optimizing process to reduce white matter retention and plan to apply the optimized compound to the candidate for an ^{18}F-labeled PET probe.

CONCLUSION

The present study demonstrated that the benzoxazole derivative BF-227 displays high binding affinity to amyloid